PHYSICAL REVIEW B **79**, 161309(R) (2009)

Electric-current-induced heat generation in a strongly interacting quantum dot in the Coulomb blockade regime

Jie Liu,[1] Juntao Song,[1] Qing-feng Sun,[1,*] and X. C. Xie[2,1]

[1]*Beijing National Laboratory for Condensed Matter Physics and Institute of Physics, Chinese Academy of Sciences, Beijing 100190, China*

[2]*Department of Physics, Oklahoma State University, Stillwater, Oklahoma 74078, USA*

(Received 16 March 2009; published 28 April 2009)

The heat generation by electric current flowing through a quantum dot with the dot containing both electron-electron interaction and electron-phonon interaction is studied. Using the nonequilibrium Keldysh Green's-function method, the current-induced heat generation is obtained. We find that for a small phonon frequency, heat generation is proportional to the current. However, for a large phonon frequency, heat generation is in general qualitatively different from the current. It is nonmonotonic with current, and many unique and interesting behaviors emerge. The heat generation could be very large in the Coulomb blockade region in which the current is very small due to the Coulomb blockade effect. On the other hand, in the resonant tunneling region, the heat generation is very small despite a large current, an ideal condition for device operation. In the curve of heat generation versus the bias, a negative differential of the heat generation is exhibited, although the current is always monotonously increasing with the bias voltage.

DOI: 10.1103/PhysRevB.79.161309 PACS number(s): 73.23.−b, 65.80.+n, 44.10.+i, 71.38.−k

With the continued miniaturization of integrated circuits, quantum phenomena and new technological problems are emerging quickly. An essential technological roadblock of this miniaturization is the "power problem." With millions of transistors assembled on a chip area no larger than a few square centimeters, the chip-level power densities may reach on the order of 100 W/cm^2. The large amount of accumulated heat caused by the current makes the chip's temperature rise to a level so high that the chip may not function properly. There are two ways to reduce the chip's temperature: one is to remove the heat as quickly as possible, while the other is to suppress the heat generation. It is unfortunate that the novel and complex device geometries normally make heat removal more difficult and most of the new materials appearing in device processing have lower thermal conductivities than bulk silicon.[1] Thus, it is essential to uncover the laws of heat generation induced by an electric current in nanoscale devices and to investigate how the heat generation may be reduced.

The idea that electric current does work on conductors and causes heating has been known since the mid-nineteenth century. It has been well studied in macroscopic systems and is known as the effect of Joule heating; however, many open questions remain concerning heating in nanoscale systems. For a net resistive nanoscale system, the total heat dissipation is still equal to the input power IV, with I being the current and V the bias voltage. In standard transport theory, such as the Landauer-Buttiker formula or the nonequilibrium Keldysh Green's-function (NEKGF) method, it is normally assumed that the electron is elastically scattered in the central region (called the scattering region) and that all heat dissipation occurs in the reservoirs.[2] This assumption does not provide a full answer to the dissipation problem. One can see this from the following two aspects: (1) if the central region contains the phonon degrees of freedom and the electron-phonon (e-p) interaction, the inelastic scattering processes and heat dissipation can occur in the central region. In this case, the simple assumption of all dissipation occurring in the reservoirs is invalid. In fact, in some recent experiments, it is found that the e-p interaction is indeed strong in some nanoscale molecular devices, such as C_{60} and nanotube.[3–5] In these devices, the phonon-assisted tunneling substeps or subpeaks have been observed in the I-V curves or in the differential conductance versus the gate voltage.[3–7] (2) Furthermore, if one wishes to investigate where and how the heat dissipation occurs while a current passes a nanodevice even assuming the device contains no e-p interaction, the e-p interactions in the leads that are near the nanodevice must also be considered. Then this part (i.e., the dissipation region) cannot be considered as a part of the reservoirs since the reservoirs are assumed to be without any interactions in the standard transport theory.

Recently, some attention has been paid to the problem of current-induced heat generation in nanoscale devices, with a few preliminary results.[8–13] Huang *et al.*[9] experimentally observed the current-induced local heating effects in single molecules by measuring the force required to break the molecule-electrode bonds. Very recently, Oron-Carl and Krupke[10] successfully determined the hot phonon generation from a current bias by using the ratio of anti-Stokes to Stokes lines. Theoretically, Lazzeri *et al.*[11] studied the heat generation in nanotube via the first-principles calculations. All previous results demonstrate that the heat generation in nanoscale devices is important. In a recent work, we studied the heat generation when an electric current passes through mesoscopic devices.[14] By using the NEKGF method, a general formula for the current-induced heat generation was derived. This formula can be applied to both the linear and nonlinear transport regions, as well the mesoscopic device with various interactions.

In this Rapid Communication, we study the current-induced heat generation while an electric current flows through a quantum dot (QD) that is in the Coulomb blockade regime, focusing on the heat transfer to the phonon part since the phonon creation is the main source of the heat generation in QD. Considering that the device consists of a QD coupled

to two leads and the QD contains the electron-electron (e-e) Coulomb interaction and e-p interaction, by using the NEKGF method and the general formula of heat generation, both the heat generation and the current are obtained. The numerical results exhibit that the heat generation in the Coulomb blockade regime has many interesting and unique behaviors. For example, (1) in the resonant tunneling region with the intradot level within the bias window, the current is very large but the current-induced heat generation is very small. This is an ideal region for the operation of the nanodevice with a large current and low heat generation. On the other hand, in the Coulomb blockade region, the current is very small but the heat generation is very large. In particular, when the e-e interaction strength is equal to the phonon frequency, a resonant phonon-emitting process occurs and a large amount of current-induced heat generation emerges, even though the current is quite small due to the Coulomb blockade effect. (2) In some parameter regions, when the bias rises, the current increases but the heat generation decreases. In other words, the negative differential of the heat generation emerges.

The system of the lead-QD-lead can be described by the following Hamiltonian:

$$H=\sum_{\alpha,k,\sigma}\varepsilon_{\alpha k}\hat{c}^{\dagger}_{\alpha k\sigma}\hat{c}_{\alpha k\sigma}+\sum_{\alpha,k,\sigma}t_{\alpha k}(\hat{d}^{\dagger}_{\sigma}\hat{c}_{\alpha k\sigma}+\mathrm{H.c.})+\omega_q\hat{a}^{\dagger}_q\hat{a}_q+\sum_{\sigma}[\varepsilon_d+\lambda_q(\hat{a}^{\dagger}_q+\hat{a}_q)]\hat{n}_{\sigma}+U\hat{n}_{\uparrow}\hat{n}_{\downarrow}, \quad (1)$$

where $\hat{n}_{\sigma}=\hat{d}^{\dagger}_{\sigma}\hat{d}_{\sigma}$ and $\alpha=L$ and R represent the left and right leads. $\hat{c}^{\dagger}_{\alpha k\sigma}$ and $\hat{d}^{\dagger}_{\sigma}$ create an electron with spin σ in the α lead and QD, respectively. Analogously, $\hat{a}^{\dagger}_q$ is the phonon creation operator and ω_q is the phonon frequency. The QD has a single energy level ε_d with the spin $\sigma=\uparrow,\downarrow$. The intradot e-e Coulomb interaction and e-p interaction are considered, with the interaction strength U and λ_q. The second term in Eq. (1) describes the tunneling coupling between the QD and the two leads, and $t_{\alpha k}$ is the hopping matrix element.

Before solving the heat generation in the QD we first make a canonical transform with the unitary operator[15] $\hat{U}=\exp\{-\Sigma_{\sigma}(\lambda_q/\omega_q)(\hat{a}^{\dagger}_q-\hat{a}_q)\hat{n}_{\sigma}\}$. After this transformation, the Hamiltonian becomes

$$\tilde{H}=\sum_{\sigma}\tilde{\varepsilon}_d\hat{d}^{\dagger}_{\sigma}\hat{d}_{\sigma}+\tilde{U}\hat{n}_{\uparrow}\hat{n}_{\downarrow}+\sum_{\alpha k,\sigma}\varepsilon_{\alpha k}\hat{c}^{\dagger}_{\alpha k\sigma}\hat{c}_{\alpha k\sigma}+\sum_{\sigma,\alpha,k}(t_{\alpha k}\hat{c}^{\dagger}_{k\sigma}\hat{d}_{\sigma}\hat{X}+\mathrm{H.c.})+\omega_q\hat{a}^{\dagger}_q\hat{a}_q, \quad (2)$$

where $\tilde{\varepsilon}_d=\varepsilon_d-\lambda^2_q/\omega_q$, $\tilde{U}=U-2\lambda^2_q/\omega_q$, and $\hat{X}=\exp\{-(\lambda_q/\omega_q)(\hat{a}^{\dagger}_q-\hat{a}_q)\}$. We make an approximation to replace the operator $\hat{X}$ by its mean value $\langle\hat{X}\rangle=\exp\{-(\lambda_q/\omega_q)^2(N_q+1/2)\}$,[15] where $N_q=1/[\exp(\omega_q/k_BT)-1]$ refers to the phonon number. This approximation was used in previous studies,[6,15] and it is known to be valid when $t_{\alpha k}\ll\lambda_q$. After taking this approximation the phonon is decoupled with the electron. Then the formula of the current-induced heat generation Q per unit time is[14]

$$Q=\mathrm{Re}\sum_{\sigma}\omega_q\lambda^2_q\int\frac{d\omega}{2\pi}\{\tilde{G}^{<}_{\sigma\sigma}(\omega)\tilde{G}^{>}_{\sigma\sigma}(\bar{\omega})-2N_q[\tilde{G}^{>}_{\sigma\sigma}(\omega)\tilde{G}^{a}_{\sigma\sigma}(\bar{\omega})+\tilde{G}^{r}_{\sigma\sigma}(\omega)\tilde{G}^{>}_{\sigma\sigma}(\bar{\omega})]\}, \quad (3)$$

where $\bar{\omega}=\omega-\omega_q$, and $\tilde{G}^{r,a,<,>}_{\sigma\sigma}(\omega)$ are the Fourier transforms of $\tilde{G}^{r,a,<,>}_{\sigma\sigma}(t)$, which are the standard QD's single-electron Green's functions of Hamiltonian (2) and are defined as $\tilde{G}^{r}_{\sigma\sigma}(t)=-i\Theta(t)\langle\{d(t),d^{\dagger}(0)\}\rangle$, $\tilde{G}^{a}_{\sigma\sigma}(t)=i\Theta(-t)\langle\{d(t),d^{\dagger}(0)\}\rangle$, $\tilde{G}^{<}_{\sigma\sigma}(t)=i\langle d^{\dagger}(0)d(t)\rangle$, and $\tilde{G}^{>}_{\sigma\sigma}(t)=-i\langle d(t)d^{\dagger}(0)\rangle$. Here heat generation Q is the dissipation in the QD region in which the energy is transferred to the local phonons. Since the present device is a net resistive system, the total dissipation is equal to the input power IV and the remaining dissipation Q_{res} occurs in the reservoirs.[16] Moreover the heat generation actually is the rate of heat generation. Hereafter we do not distinguish them because they have completely the same characteristics. Because the e-p interaction has been decoupled in Hamiltonian (2), the Green's function $\tilde{G}^{r}_{\sigma\sigma}$ can be obtained by the equation-of-motion technique as follows[2,17]:

$$\tilde{G}^{r}_{\sigma\sigma}(\omega)=\frac{[\omega_{\varepsilon}-\tilde{U}(1-\langle n_{\bar{\sigma}}\rangle)]}{\omega_{\varepsilon}(\omega_{\varepsilon}-\tilde{U})-i\tilde{\Gamma}[\omega_{\varepsilon}-\tilde{U}(1-\langle n_{\bar{\sigma}}\rangle)]}, \quad (4)$$

where $\omega_{\varepsilon}\equiv\omega-\tilde{\varepsilon}_d$, $\langle n_{\bar{\sigma}}\rangle$ is the electron occupation number in the intradot state $\bar{\sigma}$, $\bar{\sigma}=\downarrow$ while $\sigma=\uparrow$ and $\bar{\sigma}=\uparrow$ while $\sigma=\downarrow$, $\tilde{\Gamma}=(\tilde{\Gamma}_L+\tilde{\Gamma}_R)/2$, $\tilde{\Gamma}_{\alpha}=\Gamma_{\alpha}\langle X\rangle^2$, and $\Gamma_{\alpha}=\Sigma_k 2\pi|t_{\alpha k}|^2\delta(\omega-\epsilon_{\alpha k})$ is the linewidth functions which assume to be independent of the energy ω.[2,17] After solving $\tilde{G}^{r}_{\sigma\sigma}(\omega)$, $\tilde{G}^{a}_{\sigma\sigma}(\omega)=[\tilde{G}^{r}_{\sigma\sigma}(\omega)]^*$, $\tilde{G}^{<}_{\sigma\sigma}(\omega)=\tilde{G}^{r}(\omega)\tilde{\Sigma}^{<}(\omega)\tilde{G}^{a}(\omega)$, and $\tilde{G}^{>}_{\sigma\sigma}(\omega)=\tilde{G}^{<}_{\sigma\sigma}+\tilde{G}^{r}_{\sigma\sigma}-\tilde{G}^{a}_{\sigma\sigma}$, where $\tilde{\Sigma}^{<}(\omega)=i[\tilde{\Gamma}_L f_L(\omega)+\tilde{\Gamma}_R f_R(\omega)]$ and $f_{\alpha}(\omega)=1/\{\exp[(\omega-\mu_{\alpha})/k_BT]+1\}$ is the Fermi distribution function in the α lead. Substituting these Green's functions into Eq. (3), the heat generation Q can be obtained straightforwardly. Finally, the electron occupation numbers $\langle n_{\sigma}\rangle$ in Eq. (4) need to be self-consistently calculated with the equation $\langle n_{\sigma}\rangle=i\int(d\omega/2\pi)\tilde{G}^{<}_{\sigma\sigma}(\omega)$. In addition, by using the same method as in Ref. 6 the current can also be calculated.

In the numerical investigation, we consider the symmetric barriers[18] with $\tilde{\Gamma}_L=\tilde{\Gamma}_R=\tilde{\Gamma}$, and set $\tilde{\Gamma}=1$ as the unit of energy and $\mu_R=0$ as the energy zero point, then the bias $eV=\mu_L-\mu_R=\mu_L$. Figure 1(a) shows the heat generation Q and current I as functions of the bias V for the different temperature T at the QD level $\tilde{\epsilon}_d=0$. We can see that at first the heat generation Q is almost zero while the bias $V<\omega_q$ since the bias cannot offer enough energy to emit in this range. With the bias passing ω_q, both Q and I rapidly increase and reach their respective plateaus. Q and I remain at plateaus until the bias reaches $\tilde{U}$ and then they rapidly increase and reach new plateaus. The reason behind the two steps is that the QD level is split into two sublevels at $\tilde{\epsilon}_d$ and $\tilde{\epsilon}_d+\tilde{U}$ with the existence of the e-e interaction $\tilde{U}$. The temperature has little effect on the heat generation. Raising temperature makes the curves of both Q-V and I-V more smooth, but the qualitative behaviors remain. Here we emphasize that

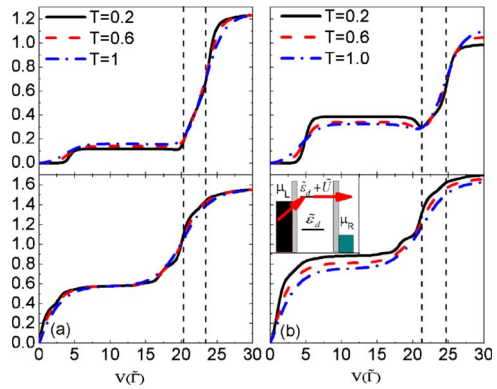

FIG. 1. (Color online) The heat generation $Q(\lambda_q^2)$ and current I vs the bias V for the different temperature T with the level (a) $\tilde{\epsilon}_d=0$ and (b) 1, and the other parameter is $\omega_q=3$, $\tilde{U}=20$, and $\lambda_q=0.6\omega_q$. The inset in (b) is schematic diagram for the tunneling process in which a phonon is absorbed.

the heat generation Q is not directly proportional to the current I, and they obviously have the following two differences: (i) many small substeps emerge in the current curves because of the phonon-assisted tunneling processes, but no phonon-assisted substeps in the heat generation curves. (ii) The rapid jumps in the current curve happen at about $V=\tilde{\epsilon}_d$ and $\tilde{\epsilon}_d+\tilde{U}$, but the rapid jumps in the heat generation curve happen at about $V=\tilde{\epsilon}_d+\omega_q$ and $\tilde{\epsilon}_d+\tilde{U}+\omega_q$, with a delay of ω_q [see Fig. 1(a)].

In Fig. 1(a), the level $\tilde{\epsilon}_d$ is fixed at zero. Next, we study the case of $\tilde{\epsilon}_d\neq 0$. Figure 1(b) describes the heat generation Q with the same parameters as in Fig. 1(a) except $\tilde{\epsilon}_d=1$. The results clearly exhibit that a negative differential heat generation dQ/dV emerges when V is between $\tilde{U}+\tilde{\epsilon}_d-\omega_q$ and $\tilde{U}+\tilde{\epsilon}_d$. In this region, with increasing V, I increases but Q decreases. The reason is that the electron can absorb as well as emit a phonon while it tunnels through the QD. When the bias V is between $\tilde{U}+\tilde{\epsilon}_d-\omega_q$ and $\tilde{U}+\tilde{\epsilon}_d$, the tunneling process as shown in the inset of Fig. 1(b) occurs in which the electron absorbs a phonon while it passes through the QD. Thus, a negative differential heat generation emerges.

Figure 2 investigates the dependence of the heat generation Q on the phonon frequency ω_q. When ω_q approaches to zero, so does the heat generation Q. With ω_q increasing from

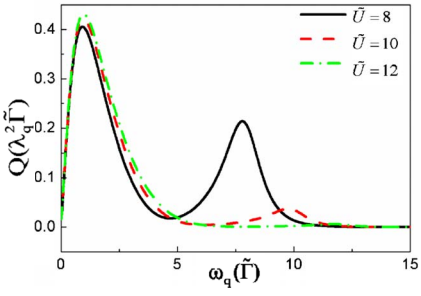

FIG. 2. (Color online) The of heat generation $Q(\lambda_q^2)$ vs the phonon frequency ω_q for different e-e interaction strength $\tilde{U}$ with the parameters: $V=4$, $T=1$, $\lambda_q=0.6\omega_q$, and $\tilde{\epsilon}_d=0$

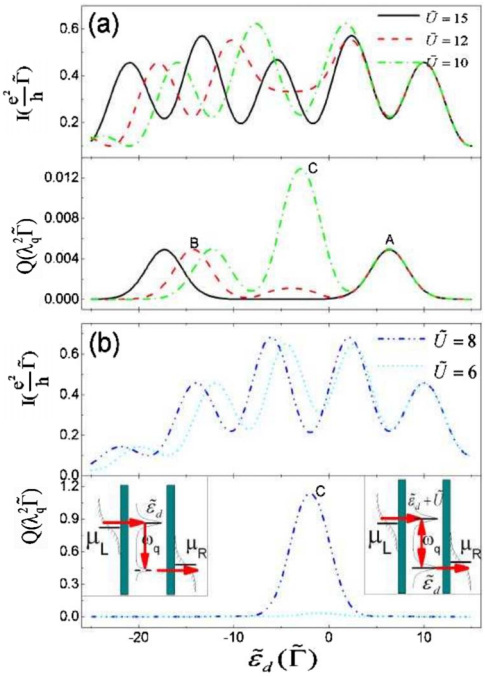

FIG. 3. (Color online) $Q(\lambda_q^2)$ and I vs the level $\tilde{\epsilon}_d$ for the different $\tilde{U}$ with the parameters $\omega_q=8$, $V=4$, $T=1$, and $\lambda_q=0.6\omega_q$. The insets in (b) are the schematic plots for two phonon-emitting processes.

zero, Q quickly increases. The curve of Q-ω_q exhibits two peaks. One peak is roughly at $\omega_q=\tilde{\Gamma}$, which is very close to zero. The other peak is at $\omega_q=\tilde{U}$. The first peak is caused by competition of two effects when raising ω_q: (1) the electron losses more energy when it emits a phonon; at the same time (2) it becomes more and more difficult to emit a phonon. The second peak is largely associated with the e-e interaction strength $\tilde{U}$. Its location is fixed at $\omega_q=\tilde{U}$, and its height strongly depends on $\tilde{U}$. The smaller $\tilde{U}$ is, the higher the peak is. In fact, this peak origins from a resonant phonon-emitting process as shown in the right inset of Fig. 3(b), which will be discussed later in more detail.

Figure 3 shows Q and I versus the QD's level $\tilde{\epsilon}_d$ for different values of the e-e interaction $\tilde{U}$. I has two main resonant peaks at $\tilde{\epsilon}_d=\bar{\mu}$ and $\tilde{\epsilon}_d+\tilde{U}=\bar{\mu}$, with $\bar{\mu}\equiv(\mu_L+\mu_R)/2$. In addition, some phonon-assisted subpeaks also emerge at the two side of the main peaks, and the distance to its main peak is $\pm n\omega_q$ $(n=1,2,3,\ldots)$. These well-known results on current have been experimentally observed.[3–5] Following, we focus on the heat generation Q. The curves of Q versus the level $\tilde{\epsilon}_d$ have three peaks, which are marked "A," "B," and "C." Peak "A" ("B") stands at the valley between the right (left) main peak and its right-side (left-side) subpeak of the current. Peak "C" places at $\tilde{\epsilon}_d+\tilde{U}/2=\bar{\mu}$, i.e., at the valley (the Coulomb blockade region) between the two main peaks of the current. Here we emphasize that none of the peaks of Q aligns with that of I. In fact all peaks of Q appear at the valleys of I. This means that the heat generation is small for large current and vice versa. Here we also emphasize another important feature:

with the e-e interaction $\tilde{U}$ approaching to the phonon frequency ω_q, peak "C" is greatly enhanced. At $\tilde{U}=\omega_q$, peak "C" is very large. For example, peak "C" in Fig. 3(b) with $\tilde{U}=\omega_q=8$ is hundredfold higher than peak "C" in Fig. 3(a) with $\tilde{U}=10$. Due to the largeness of peak "C," peaks "A" and "B" are not visible in Fig. 3(b), although they are there. As far as for the current, there is no such high peak at all.

Let us explain why the heat generation Q is large at the valleys of the current. This is because the phonon-emitting processes are stronger in the current valley region. For example, to consider the phonon-emitting tunneling process in the left inset of Fig. 3(b) in which an electron from the left lead tunnels into the QD at the level $\tilde{\epsilon}_d$, emits a phonon and jumps to the sublevel $\tilde{\epsilon}_d-\omega_q$ due to the e-p interaction, and then tunnels to the right lead. The strength of this process is direct ratio of the occupation probability $f_L(\tilde{\epsilon}_d)$ of the left lead at the energy $\omega=\tilde{\epsilon}_d$ and the empty probability $1-f_R(\tilde{\epsilon}_d-\omega_q)$ of the right lead at the energy $\omega=\tilde{\epsilon}_d-\omega_q$. So this process is maximum at $\tilde{\epsilon}_d-\omega_q/2=\bar{\mu}$ and leads to peak "A" in the curve of Q-$\tilde{\epsilon}_d$. The origin of peak "B" is same as for peak "A." Peak "C" originates from the tunneling process as shown in the right inset of Fig. 3(b), which is similar to that in the left inset of Fig. 3(b). But the two levels $\tilde{\epsilon}_d$ and $\tilde{\epsilon}_d+\tilde{U}$ are real electronic levels now. Therefore the resonant phonon emitting occurs when the difference $(\tilde{U})$ of two levels is equal to the phonon frequency ω_q, giving rise to a huge peak in heat generation.

Finally, in Fig. 4 we present the contour plot of the heat generation Q and current I versus the QD level $\tilde{\epsilon}_d$ and phonon frequency ω_q. As ω_q approaches to zero, Q also approaches to zero regardless of the other parameters; however, I can be large if the resonant tunneling occurs. At small but nonzero ω_q, e.g., $\omega_q<\tilde{\Gamma}$, the heat generation Q is approximately proportional to the current I. In this case the quantum result of the heat generation resembles the classical one. On the other hand, at large ω_q (e.g., $\omega_q>\tilde{\Gamma}$), the contour of the heat generation is totally different from the contour of the current. For example, for $\omega_q=\tilde{U}$, a great heat generation appears, but we cannot find any large change in the current plot.

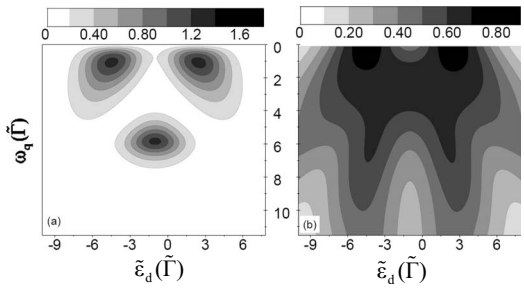

FIG. 4. (a) $Q(\lambda_q^2)$ and (b) I vs the level $\tilde{\epsilon}_d$ and phonon frequency ω_q with $\tilde{U}=6$, $V=4$, $T=1$, and $\lambda_q=0.6\omega_q$

In summary, we investigated the heat generation in a QD under a bias and in the Coulomb blockade regime. The results show that for the small phonon frequency, the heat generation is proportional to the current. On the other hand, for the large phonon frequency, the heat generation is quite different from the current and exhibits many unique and interesting characteristics. For instance, a negative differential heat generation emerges in some parameter regions even though the differential conductance is always positive. In particular, the heat generation is large in the Coulomb blockade region, while it is small in the resonant tunneling region. The later behavior is advantageous for the QD device because the QD device normally works in the resonant tunneling region and low heat generation is ideal for device operation.

We gratefully acknowledge the financial support from the Chinese Academy of Sciences, NSF-China under Grants No. 10525418, No. 10734110, and No. 10821403 and National Basic Research Program of China (973 Program Project No. 2009CB929100). X.C.X. is supported by U.S.-DOE under Grant No. DE-FG02- 04ER46124 and C-SPIN center in Oklahoma.

*sunqf@aphy.iphy.ac.cn

[1] E. Pop *et al.*, Proc. IEEE **94**, 1587 (2006).
[2] H. Haug and A. P. Jauho, *Quantum Kinetics in Transport and Optics of Semiconductors* (Springer Verlag, Berlin, 1998); S. Datta, *Electronic Transport in Mesoscopic Systems* (Cambridge University Press, Cambridge, England, 1995).
[3] H. Park *et al.*, Nature (London) **407**, 57 (2000).
[4] B. J. Leroy *et al.*, Nature (London) **432**, 371 (2004); B. J. LeRoy *et al.*, Phys. Rev. B **72**, 075413 (2005).
[5] S. Sapmaz *et al.*, Phys. Rev. Lett. **96**, 026801 (2006).
[6] Z. Z. Chen *et al.*, Phys. Rev. B **71**, 165324 (2005).
[7] N. S. Wingreen *et al.*, Phys. Rev. B **40**, 11834 (1989); U. Lundin and R. H. McKenzie, *ibid.* **66**, 075303 (2002); A. Mitra *et al.*, *ibid.* **69**, 245302 (2004); D. A. Ryndyk and J. Keller, *ibid.* **71**, 073305 (2005); L. E. F. Foa Torres, *ibid.* **72**, 245339 (2005); H. M. Pastawski *et al.*, Chem. Phys. **281**, 257 (2002).
[8] A. P. Horsfield *et al.*, Rep. Prog. Phys. **69**, 1195 (2006).
[9] Z. Huang *et al.*, Nano Lett. **6**, 1240 (2006); Z. Huang *et al.*, Nat. Nanotechnol. **2**, 698 (2007).
[10] M. Oron-Carl and R. Krupke, Phys. Rev. Lett. **100**, 127401 (2008).
[11] M. Lazzeri *et al.*, Phys. Rev. Lett. **95**, 236802 (2005).
[12] M. J. Montgomery *et al.*, J. Phys.: Condens. Matter **14**, 5377 (2002); Y.-C. Chen *et al.*, Nano Lett. **3**, 1691 (2003); **5**, 621 (2005).
[13] M. Galperin *et al.*, Phys. Rev. B **75**, 155312 (2007); J. T. Lu and J.-S. Wang, *ibid.* **76**, 165418 (2007).
[14] Q.-f. Sun and X. C. Xie, Phys. Rev. B **75**, 155306 (2007).
[15] G. D. Mahan, *Many-Partical Physics* (Plenum, New York, 1990); A. Hewson and D. Newns, J. Phys. C **13**, 4477 (1980).
[16] Notice that Q can be larger than IV although $Q+Q_{\rm res}=IV$. For example, in the Fig. 3(b) $Q\approx 1.14\lambda_q^2$ at the highest point of the peak "C," which is greatly larger than $IV\approx 0.215\times 4$.
[17] A. Groshev *et al.*, Phys. Rev. Lett. **66**, 1082 (1991); Q.-F. Sun and X. C. Xie, Phys. Rev. B **73**, 235301 (2006).
[18] For the nonsymmetric barriers, the heat generation Q is directly proportion to the value in the symmetric case; thus, all results remain the same.